REPORT DOCUMENTATION PAGE

Form Approved
OMB No. 0704-0188

1. REPORT DATE *(DD-MM-YYYY)*	2. REPORT TYPE	3. DATES COVERED *(From - To)*
	Technical Paper	

4. TITLE AND SUBTITLE

5a. CONTRACT NUMBER
F04611-01-C-0010

5b. GRANT NUMBER

5c. PROGRAM ELEMENT NUMBER

6. AUTHOR(S)

5d. PROJECT NUMBER
BMDO

5e. TASK NUMBER
SBRU

5f. WORK UNIT NUMBER

7. PERFORMING ORGANIZATION NAME(S) AND ADDRESS(ES)

8. PERFORMING ORGANIZATION REPORT

9. SPONSORING / MONITORING AGENCY NAME(S) AND ADDRESS(ES)

Air Force Research Laboratory (AFMC)
AFRL/PRS
5 Pollux Drive
Edwards AFB CA 93524-7048

10. SPONSOR/MONITOR'S ACRONYM(S)

11. SPONSOR/MONITOR'S NUMBER(S)

12. DISTRIBUTION / AVAILABILITY STATEMENT

Approved for public release; distribution unlimited.

13. SUPPLEMENTARY NOTES

14. ABSTRACT

15. SUBJECT TERMS

16. SECURITY CLASSIFICATION OF:			17. LIMITATION OF ABSTRACT	18. NUMBER OF PAGES	19a. NAME OF RESPONSIBLE PERSON
a. REPORT	b. ABSTRACT	c. THIS PAGE			Leilani Richardson
Unclassified	Unclassified	Unclassified	A		19b. TELEPHONE NUMBER *(include area code)* (661) 275-5015

4 separate items are enclosed

BMDO SBIR 01-C-0010 DTS

MEMORANDUM FOR PRS (Contractor Publication)

22 March 2002

FROM: PROI (STINFO)

SUBJECT: Authorization for Release of Technical Information, Control Number: **AFRL-PR-ED-TP-2002-069**
Muss et al. (Sierra Engineering), "Swirl Coaxial Injector Development Part I Test Results"

(Statement A)

Rich 56177

JANNAF Joint Propulsion Meeting
(Destin, FL, 8-12 April 2002) (Deadline: 08 April 02)

CL 02-069

SWIRL COAXIAL INJECTOR DEVELOPMENT PART I – TEST AND RESULTS

J.A. Muss and C.W. Johnson
Sierra Engineering Inc., Carson City, NV

R.K. Cohn, P.A. Strakey, R.W. Bates and D.G. Talley
Air Force Research Laboratory, Edwards AFB, CA

ABSTRACT

Sierra Engineering, in conjunction with the Air Force Research Laboratory Propulsion Directorate, has undertaken a program to develop a gas-centered, swirl coaxial injector. This injector design will be used in the multi-element Advanced Fuels Tester (AFT) engine to test a variety of hydrocarbon propellants. As part of this program, a design methodology is being developed which will be applicable to future injector design efforts. The methodology combines cold flow data, acquired in the AFRL High Pressure Injector Flow facility, uni-element hot fire data, collected in AFRL Test Cell EC-1, and a computational effort conducted at University of Alabama-Birmingham, to identify key design features and sensitivities. Results from the computational effort will be presented in the Part II companion paper (9).

Three different gas-centered swirl coaxial element concepts were studied: a converging design, a diverging design, and a pre-filming design. The cold flow experiments demonstrated that all three classes of elements produced an extremely dense, solid cone spray, with the highest mass density in the center. The atomization of all of these injectors was excellent, producing mean drop sizes 1/3 to 1/4 of that typically measured for shear coaxial elements operating under similar conditions. Uni-element hot fire testing of these elements has begun, but the elements have not yet been tested at the design operating conditions. Preliminary low chamber pressure test results show the converging design performs better than the pre-filming and diverging design. Uni-element C* efficiencies in excess of 90% have been measured over a wide-range of mixture ratios.

INTRODUCTION

Sierra Engineering is developing a small combustion chamber for testing alternative hydrocarbon fuels for the Air Force Research Laboratory (1). The Advanced Fuels Tester (AFT) is designed to operate with gaseous oxygen (GOX) as an oxidizer and a variety of hydrocarbon fuels. The design chamber pressure is 750 to 1500 psia without changes to the combustor throat or injection element. Thrust varies with chamber pressure from 1000 lb_f to 2000 lb_f in the device. The nominal engine operating oxidizer-to-fuel mixture ratio (MR) is specified as the MR that produces peak specific impulse (ISP) at a 40:1 expansion ratio. Therefore the nominal MR varies with fuel, but most fuels of interest result in a nominal MR of about 2.7. Additionally, the injector should be insensitive to MR excursions between -20% and +10% of the nominal value.

The AFT hardware design includes a gas-centered swirl coaxial injector element similar, in principle, to the injection element used in many Russian flight engines. As the name implies, this element concept directs the gaseous propellant (GOX) through the center of the element with the liquid propellant injected along the periphery of the element. The liquid propellant is injected tangentially along the element wall, producing a swirling liquid film. The gas-centered swirl coaxial injection element differs from the swirl coaxial elements previously demonstrated by Aerojet (2) and Pratt & Whitney (3), amongst others, in that these latter designs swirl the central liquid propellant and shroud the liquid with a coaxially injected gas. The gaseous propellant may also include a swirl component in these designs.

The motivation for the radically different injector design approach can be found in basic combustion chemistry. Previous domestic (USA) applications of swirl coaxial injectors to rocket engines have been primarily to gaseous fuel/liquid oxidizer systems; as such the approach was to shroud the liquid oxidizer with gaseous fuel, the oxidizer, in theory, will be completely encapsulated, and ultimately consumed by the gaseous fuel. This prevents free oxidizer from reaching the combustion chamber wall. In contrast, the AFT hardware, as well as the Russian engines that employ the gas-centered injection element, utilizes a gaseous oxidizer and liquid fuel. Therefore, the gas-centered swirl coaxial injector also encapsulates the oxidizer with fuel. In both cases, atomization of the liquid propellant is accomplished through a combination of conventional swirl atomization, i.e., thinning of a liquid sheet until surface instabilities initiate ligamentation and ultimately atomization, and shear induced by the high-speed adjacent gaseous propellant.

The gas-centered swirl coaxial element also offers potential to increase the thrust-per-element which can potentially reduce both fabrication and operating costs. The largest US oxygen-hydrocarbon engines, which utilize conventional impinging elements, achieve a thrust-per-element on the order of 2,500 lb_f (4). In contrast, the Russian RD-170 engine, utilizing this typeof element, has a thrust-per-element in excess of 6,000 lb_f.

While the gas-centered swirl coaxial injector appears to be well suited for the AFT and other future oxygen-hydrocarbon applications, there is a dearth of design guidelines and test data for this type of element in the US. Liquid swirl-type injectors are commonly used in industrial applications that include industrial boilers, gas turbines and spray drying. They have also been the subject of numerous design monographs, such as References 5 and 6. However, these applications address sprays into a quiescent or co-flowing gas, with the gas typically being the oxidizer. This application is more consistent with the traditional liquid-centered swirl coaxial design. Lefebvre describes several applications where gas is introduced on both the inside and outside of the liquid fuel sheet with the intention of enhancing atomization (5), but, as noted above, this application is designed to uniformly distribute the liquid spray within the gaseous oxidizer. These approaches can give some guidance to the design and operating characteristics of a gas-centered swirl coaxial injector, but it is not directly applicable design data.

Sierra Engineering has joined with the Air Force Research Laboratory, Propulsion Directorate, Aerophysics Branch (AFRL/PRSA) to systematically investigate the sensitivity of various design parameters on the operating characteristics of gas-centered swirl coaxial injection elements. The program utilizes a combination of uni-element cold flow and uni-element hot fire tests along with computational fluid dynamic (CFD) calculations, to develop a design approach for the AFT injector element. The following sections describe the test hardware designs, the cold flow test results, and preliminary hot fire test results. The results of the CFD calculations are discussed in the companion paper (9).

HARDWARE DESIGN

The AFT hardware is designed to be a workhorse set of hardware with the ability to test a variety of propellants. It is designed in a modular fashion to easily allow changes in the hardware such as the injector to gain the best results. The hardware is designed to produce a thrust of 2000 lb_f at a chamber pressure of 1500 psia. In order to examine the effects of inter-element mixing, it was decided to use five 400 lb_f thrust elements in order rather than a single 2000 lb_f element. The element quantity was chosen to maximize the element thrust while providing a moderately symmetric wall condition. The baseline fuel for the AFT hardware is ambient temperature n-butane (C_4H_{10}), with a nominal operating MR of 2.8. The goal for the AFT injector is to provide high combustion efficiency (>97%), along with stable combustion, reasonably uniform wall conditions and good face compatibility. The injector itself must also be durable and operate with modest injection pressure drops. Thus there can not be appreciable burning in the element.

The basic gas-centered swirl coaxial element design can be conceptualized as a straight-run post for the oxidizer. The post includes a discrete set of fuel injection orifices near the downstream exit of the oxidizer post. The orifices are oriented to generate swirling fuel around the periphery. The fuel film generated around the post periphery is subject to a combination of cross-flow shear and centrifugal forces. As the liquid exits the tip of the oxidizer post, centrifugal forces create a conically expanding sheet of liquid that thins due to continuity. This liquid sheet film also interacts with the central oxygen gas jet, which typically entrains the liquid fluid, transporting the resultant spray downstream. The parameters that can be varied in this design include the number of fuel injection orifices, the axial location of the orifices relative to the final injection location and most importantly the post geometry near the fuel injection orifices. Three basic injector concepts were identified for comparative evaluation, the diverger, the converger and the pre-filmer, as shown schematically in Figure 1, Figure 2 and Figure 3, respectively.

The diverger design injects the fuel downstream of a sudden expansion, with the expansion having a characteristic expansion angle. The characterized dimensions of the diverger, shown in Figure 1, are the oxidizer post diameter (A), the diameter of the sudden expansion (E), the length of the expansion section (C) and the divergence angle (θ). Additional parameters are the diameter (D) and quantity of fuel injection orifices. Several of these characteristic dimensions should also be considered as ratios: the expansion ratio (E/A), expansion distance

(C/A) and the fuel orifice diameter to expansion step (2D/[E-A]). A set of five parametric diverger element designs was developed, as described in Table 1.

The converger element design is loosely based on the main chamber injection element used in several Russian staged-combustion engines. The fuel is tangentially injected into the main oxidizer post. Then, the post necks-down to accelerate both the liquid and gaseous flows. The characterized dimensions of the converger, shown in Figure 2, are the oxidizer post diameter (A) and the diameter (E) and length (C) of the necked-down section. Again, additional parameters are the diameter (D) and quantity of fuel injection orifices. The characteristic dimensions that should be considered as ratios are the contraction ratio (E/A) and the interaction distance (C/A). A set of four parametric converger element designs was developed as described in Table 1.

The pre-filmer element is an adaptation of designs commonly used in gas turbines and industrial boilers (5). The liquid fuel is injected tangentially into a recessed groove (Figure 3). The axial dimension of the groove should be large enough to permit the liquid film to homogenize before being exposed to the high-speed gaseous core flow. The film is then circumferentially accelerated as the groove diameter narrows to the main gas port diameter. The characterized dimensions of the pre-filmer are the oxidizer post diameter (A), the diameter (E) and length (F) of the pre-filming groove and the length of the interaction section (C). The diameter (D) and quantity of fuel injection orifices are important, as with the other designs. The key characteristic ratio to be considered is the interaction distance (C/A), although the ratio between the oxidizer post diameter and the dimensions of the pre-filmer groove (E and F) may also be important. Only two parametric pre-filmer element designs were developed as described in Table 1.

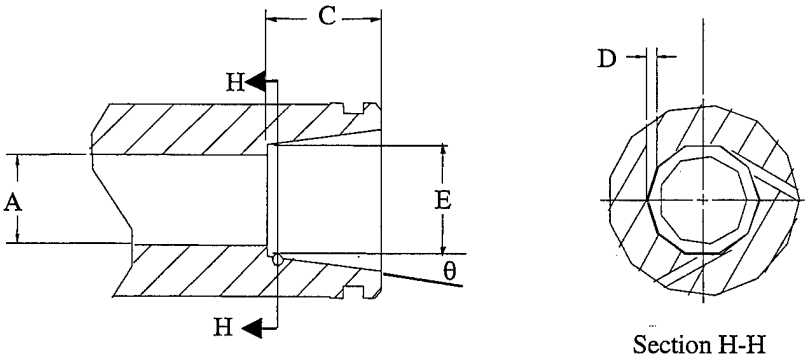

Figure 1: Schematic of Diverger Gas-Centered Swirl Coaxial Injector

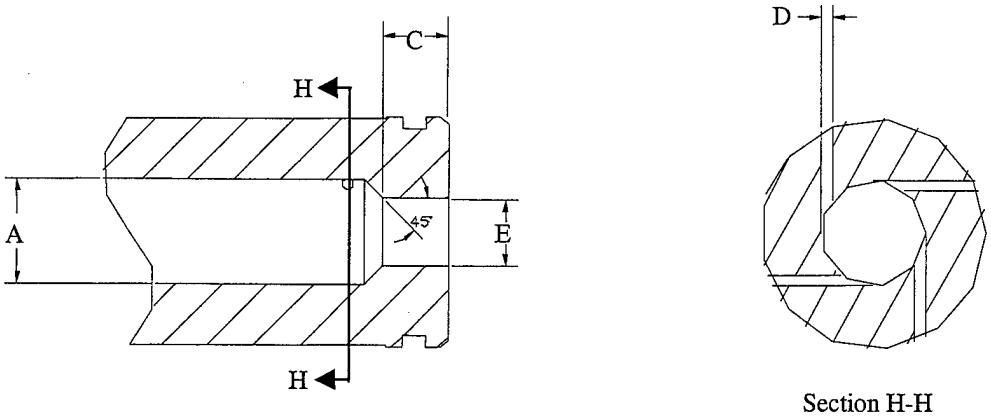

Figure 2: Schematic of Converger Gas-Centered Swirl Coaxial Injector

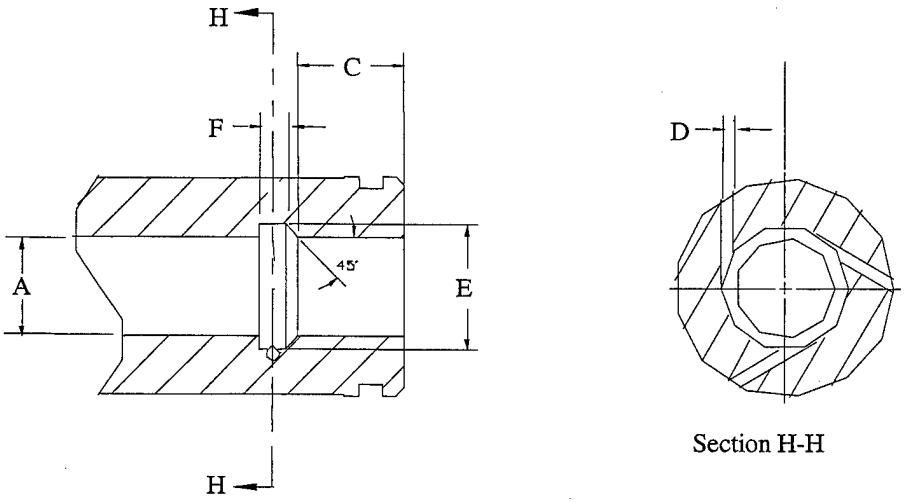

Figure 3: Schematic of Pre-filmer Gas-Centered Swirl Coaxial Injector

Table 1: Characteristic Dimension of Elements (in inches)

DASH #	TYPE	A	C	θ (deg)	D	E	F
1	Diverger	0.400	0.525	0	3 @ 0.047	0.503	-
2	Diverger	0.400	0.525	7	3 @ 0.047	0.503	-
3	Diverger	0.400	0.525	13.65	3 @ 0.047	0.503	-
4	Diverger	0.400	0.325	0	3 @ 0.047	0.503	-
5	Diverger	0.250	0.375	0	3 @ 0.047	0.353	-
6	Pre-filmer	0.400	0.400	-	3 @ 0.047	0.503	0.103
7	Pre-filmer	0.400	0.200	-	3 @ 0.047	0.503	0.103
8	Converger	0.400	0.250	-	3 @ 0.047	0.250	-
9	Converger	0.400	0.250	-	3 @ 0.047	0.125	-
10	Converger	0.400	0.250	-	4 @ 0.041	0.250	-
11	Converger	0.400	0.325	-	3 @ 0.047	0.250	

The parametric element designs were developed using some simple common constraints. The nominal fuel injection pressure drop was set at 20% of the chamber pressure, i.e. 300 psid. This value was chosen to ensure that the fuel injection process was decoupled from the combustion process. In order to keep the nominal fuel injection pressure drop constant, the fuel injection orifice diameter changed as the fuel injection orifice quantity varied. The oxidizer post inlet diameter was selected so the nominal GOX velocity was approximately 200 ft/s. This value was selected to reduce the likelihood of fires initiated by particle-impact in the high pressure GOX system. Subsequent analyses have shown that this value was too low, since it resulted in low injection pressure drops (20-30 psid) in many of the injector designs.

The subject uni-element testing used full-scale AFT element concepts (400 lb_f) integrated into the AFRL uni-element test rig. Cold flow testing was performed in the Area 1-14 High Pressure Cold-Flow Facility while hot fire testing was performed in EC-1 using a workhorse uni-element test rig. This heat-sink design (Figure 4) is based on the Penn State University uni-element diagnostic engine design. The design includes several modular segments held together in a hydraulic ram. The segments include the injector, windowed test segment, barrel extension segment with igniter, two additional barrel segments and the convergent-divergent nozzle segment (from left to right in Figure 4). The windowed section has been replaced with a straight spacer section during these initial characterization experiments. Future experiments are planned using the windowed section to gain access to the interior engine flow characteristics. Ignition is achieved using a hydrogen-oxygen torch that does not run during main-stage engine operation.

A benefit of this engine design is that engine length (L') changes are very straight forward. The majority of testing, including all of the results presented in this paper, have been conducted with L'=7 in.

The interior cross-section of this engine is a 2 inch square. This large chamber facilitates access for optical diagnostic; however, it also result in an extremely large contraction ratio ($A_{chamber}/A_{throat} = 26$).

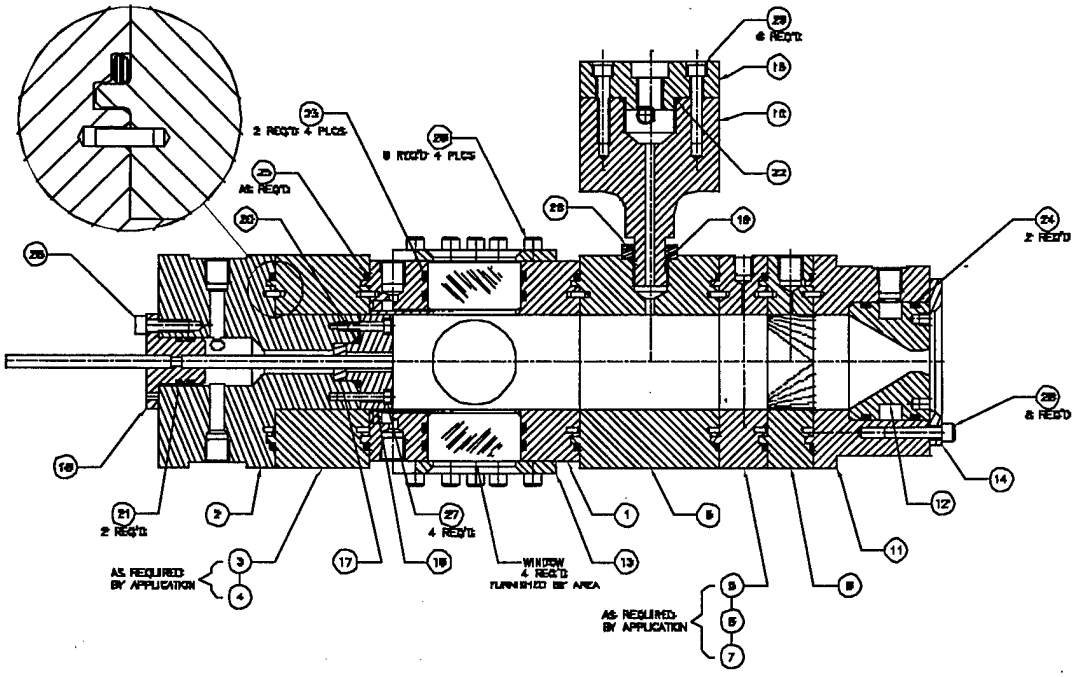

Figure 4: Basic Layout of EC-1 Uni-Element Test Rig

In order to facilitate testing, Sierra Engineering designed an alternative injector segment that could be used in both the EC-1 test rig and the 1-14 High Pressure Cold-Flow facility. The injector assembly includes a copper injector body and oxidizer manifold closeout, a copper test element and a nickel 200 retainer plate. Monel 400 fittings and Viton o-rings were used on the oxidizer system for GOX compatibility. External ports are included to feed the propellants and measure the oxidizer feed pressure.

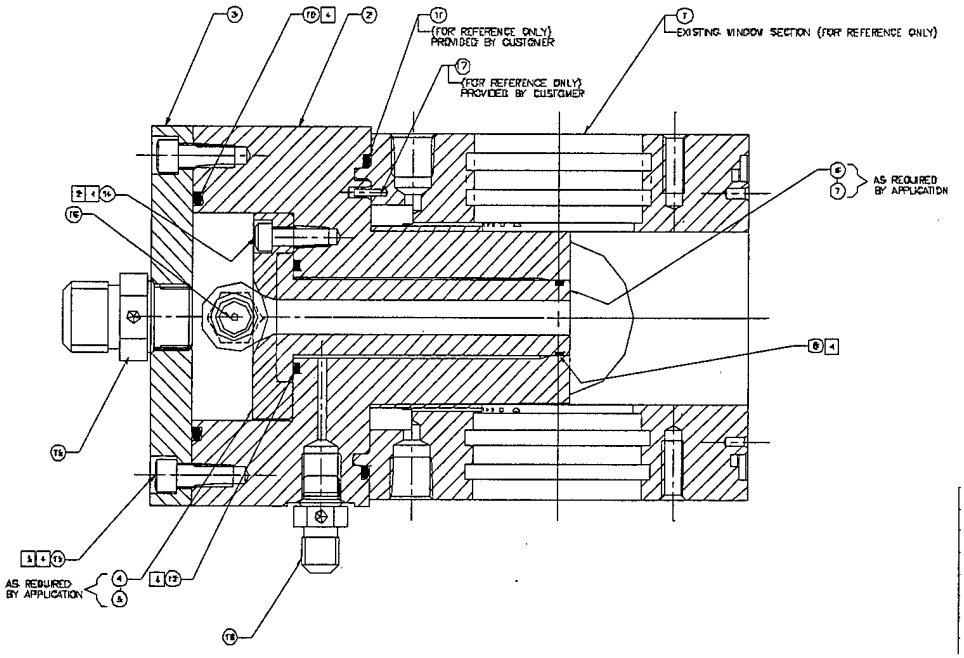

Figure 5: Detail of Sierra Uni-Element Test Injector Assembly

COLD FLOW TEST RESULTS

Cold flow testing was performed at the AFRL High Pressure Cold-Flow Facility located in Area 1-14 at Edwards AFB. The testing used water to simulate the liquid fuel gaseous nitrogen to simulate GOX. The cold flow tests were performed in a vessel pressurized with gaseous nitrogen. The vessel design allows the back-pressure to be adjusted and includes windows for optical access. The diagnostics utilized for this study included back-lit strobe imaging of the spray, mechanical patternation for measurement of liquid flux distribution and phase Doppler interferometry for droplet size and velocity measurement. The mechanical patternator in this system is a linear array, but the injector can be rotated and traversed across the patternator to fully characterize the circumferential spray distribution generated by an injector element. The axial station for all diagnostics can be varied between 1 and 6 inches downstream of the injector exit, although most of the subject test data was collected at 2.0 inches downstream of the injector exit.

The cold flow test conditions were designed to simulate the hot fire operating conditions with respect to the propellant conditions at the point of injection. The cold flow injector operating conditions were designed to match to the hot fire operating condition in the following manner. First, the liquid injection velocity was set to the corresponding hot fire operating condition. Second, the injected gas density was matched to the hot fire operating condition based on chamber back-pressure. Since the density of ambient temperature nitrogen and oxygen are very similar, the second condition is achieved with only a slight variation in chamber back-pressure relative to the hot fire chamber pressure. With fuel injection velocity and oxidizer density equivalent to the hot fire case, the final adjustment was to match the hot fire gas-to-liquid momentum ratio by adjusting the mass flow rate of gaseous nitrogen. Using the above matching conditions, the injectors were tested at chamber pressures ranging from 286 to 1143 psia. These pressures correspond to 250 psia and 100 psia hot-fire conditions. Selected elements were also tested over a range of injected mixture ratios. The cold flow analog to the 1500 psia hot fire chamber pressure, 1715 psia, was not tested. A comparison of several hot fire operating conditions and the analogous cold flow simulation operating conditions is included as Table 2.

Table 2: Comparison of Element Operating Conditions, Hot Fire to Cold Flow

Hot Fire Operating Conditions								Cold Flow Simulation			
Pc (psia)	Fvac (lb_f)	Mox (lb/s)	Mf (lb/s)	Voj (ft/s)	Vfj (ft/s)	mVo/mV_f	Vo/V_f	Pc (psia)	M_{H2O} (gpm)	Voj (ft/s)	M_{N2} (lb/s)
250	333	0.86	0.27	199	55.5	11.46	3.6	286	0.67	254.9	0.31
500	667	1.72	0.54	199	111	5.73	1.8	572	1.34	254.9	0.62
750	1000	2.57	0.80	199	167	3.81	1.2	857	2.01	255.4	0.93
1000	1333	3.43	1.07	199	222	2.87	0.9	1143	2.68	255.1	1.24
1500	2000	5.15	1.61	199	333	1.91	0.6	1715	4.02	254.9	1.86

It should be noted that all of the chamber pressures examined in the cold flow testing are subcritical relative to the fuel stimulant (water); however, many of the hot fire operating conditions are supercritical relative to the actual fuels planned for the AFT tests. Because of the difference in the properties of sprays and jets under subcritical and supercritical conditions, one must be careful in the interpretation of these results. Under supercritical conditions, droplets do not exist. However, it is believed that droplet sizes measured under subcritical conditions correspond to the size of structural features found in supercritical conditions. Thus, smaller drop sizes in the subcritical conditions will correspond to smaller structural length scales under supercritical conditions. This will result in an increase in the amount of surface area available for mixing to occur. It is also likely that the mass flux distribution pattern measured in the subcritical, cold flow tests will have a smaller spatial distribution, i.e., there will be less smearing, than would under supercritical conditions. Similar results have been seen in Chehroudi *et al.* (8) where it was found that the spreading rate of a supercritical jet is significantly larger than that for subcritical jets. The increased spreading rate, combined with the lack of a latent heat of vaporization in the supercritical condition will likely yield an increase in mixing over the subcritical case.

Eight of the eleven candidate elements were successfully cold flow tested over a range of operating pressures. The other three elements were not tested because of either element machining problems or diagnostic limitations of the facility.

Several different measurements were made of each element's performance characteristics, some qualitative and others quantitative. Back-lit strobe images were used to qualitatively compare the near-field spray patterns of the different injection elements. Tests were run with only the liquid circuit operating and then with both fluid circuits operating. The "liquid only" tests produced a rapidly expanding liquid cone. The cone typically expanded with half-angles exceeding 75° and often wet the injector face plate. However, when the gas and liquid circuits were run simultaneously, the free liquid film was pulled inwards towards the gas core and rapidly entrained. The images for the 333 lb_f equivalent operating condition are presented in Figure 6. The diverger elements (#1, #3 and #4), appear to have a wider spray pattern with relatively large liquid droplets being thrown toward the periphery of the spray, while the pre-filmer and converger elements produce a narrower spray cone with what appears to be finer droplet sizes.

More quantitative measurements were performed using a combination of mechanical patternation and phase Doppler velocimetry. The patternator was designed to measure the axial component of the liquid flux using a linear array of 27 tubes, each 1/4" square. The liquid (and gas) entering the patternator tubes drain into collection bottles where the liquid level was measured using a capacitance probe accurate to ± 2%. Although the gas vents off to a common manifold that connects back to the chamber, the pressure drop through the patternation system only allows about 25% of the gas to pass through the tubes. This generated a partial stagnation region at the entrance of the patternator tubes and prevented some of the smaller droplets from entering the tubes. The larger droplets have enough momentum to pass through the streamlines and enter the tubes. The collection efficiency of the patternator was defined as the ratio of the integrated liquid mass flux to the injected liquid flow rate. The high gas flow rates and injection velocities generated by these swirl coaxial elements combined with the small droplet sizes resulted in measured collection efficiencies were much less than 100%. The measured collection efficiencies were in the range of 22% - 65%.

Droplet size and velocity were measured using a laser-based phase Doppler interferometer. The instrument simultaneously measures the size and velocity of individual droplets as they pass through a 60 μm by 75 μm probe volume. The optical configuration in this experiment was set to measure droplet sizes ranging from 3.8 μm to 440 μm and velocities ranging from -50 m/s to 250 m/s. The average velocity of droplets less than 20 μm in diameter

was taken as a good estimate of the average gas-phase velocity (7). The extreme density of the spray prevented phase Doppler measurements at element flows above equivalent thrusts of 333 lb_f. Even at this flow condition data validation rates for droplet sizing were as low as 15% in the center of the spray, where the liquid mass flux was the highest. In comparison, data validation rates as high as 90% were achieved at the edges of the spray. The validation rates for the velocity measurements were much larger than those for the droplet sizing, typically greater than 97% throughout the spray.

In order to account for the low collection efficiency of the mechanical patternator, the raw liquid mass flux data were scaled according to the measured collection efficiency for each radial profile. For example, if the collection efficiency was 50%, the liquid flux data were multiplied by a factor of 2. Radial profiles of liquid mass flux (measured with the patternator) and axial gas velocity measured at 2.0 inches downstream of the injection point are displayed in Figure 7. The patternator collection efficiency is annotated on each plot. All of the sprays appear to have a solid-cone structure with both the gas and liquid circuits flowing. The diverger elements (#1, #3 and #4) generated a significantly wider spray pattern than the converger elements (#8 and #11). The pre-filmer elements tended to generate a more moderate spray pattern in terms of radial spreading rate. These results are consistent with the imaging experiments discussed earlier (Figure 6).

Most of the mass flux patterns appeared to be well behaved, reaching a maximum value at the centerline and falling off with an approximately Gaussian distribution (Figure 8). One exception was the 15° diverger element (#3) that showed a significant asymmetry in the liquid flux distribution. The extent of the asymmetry in the liquid flux of Element #3 was later documented with a series of patternator tests at different circumferential positions at a back-pressure of 857 psia (Figure 8). The symmetry of the liquid flux distribution for Element #3 improved with increasing back-pressure for all of mixture ratios tested.

A comparison of mean droplet size at the centerline of the spray for the eight elements tested at the 333 lb_f equivalent flow condition is shown in Figure 9. All elements exhibited excellent atomization characteristics, producing mean drop sizes 3 to 4 times smaller than shear coaxial elements operating under similar conditions. The volume mean droplet diameter (D_{43}) ranged from 50 to 70 μm while the number mean droplet diameter (D_{10}) ranged from 25 to 40 μm (Figure 9).

The final data collected during the cold flow testing phase were gas and liquid pressure drops across the injection elements. The goal was to assess the effect of the various element geometries on the injector pressure drop. It was realized early in the testing that the oxidizer (gas) manifold velocity was relatively high, and in some cases, comparable to the gas velocity in the GOX post. Therefore, the measured manifold pressure was not a stagnation value, but a static pressure measurement. In spite of this, the data is still qualitatively informative in terms of relative pressure drop for the various element designs (Figure 10). As expected, the gas-side pressure drop was much higher for the converger injection elements (#8, #9 and #11). Also, because the liquid injection holes were located upstream of the converging section, the required liquid manifold supply pressure was much higher than the pre-filmer or diverger designs. These data raised concerns about potentially strong coupling between the converger element gas and liquid circuits during hot fire testing.

The conclusions of the cold flow testing, which guided the selection of elements for the initial hot fire testing, were that the element designs were more alike than different. All element designs produced sprays that were hollow-cone with only liquid flowing, but became solid-cone sprays with both gas and liquid circuits flowing. Additionally, the atomization characteristics of all injectors were excellent, producing small droplet sizes relative to comparable shear coaxial injectors. Except for #3, the injection element concepts produced sprays with adequate symmetry. The diverger and pre-filmer elements provided greater radial spreading of the liquid spray than the converger elements. It was believed that this characteristic could result in improved inter-element mixing and flame-holding during hot fire tests. The diverger elements also had modest injection pressure drop requirements.

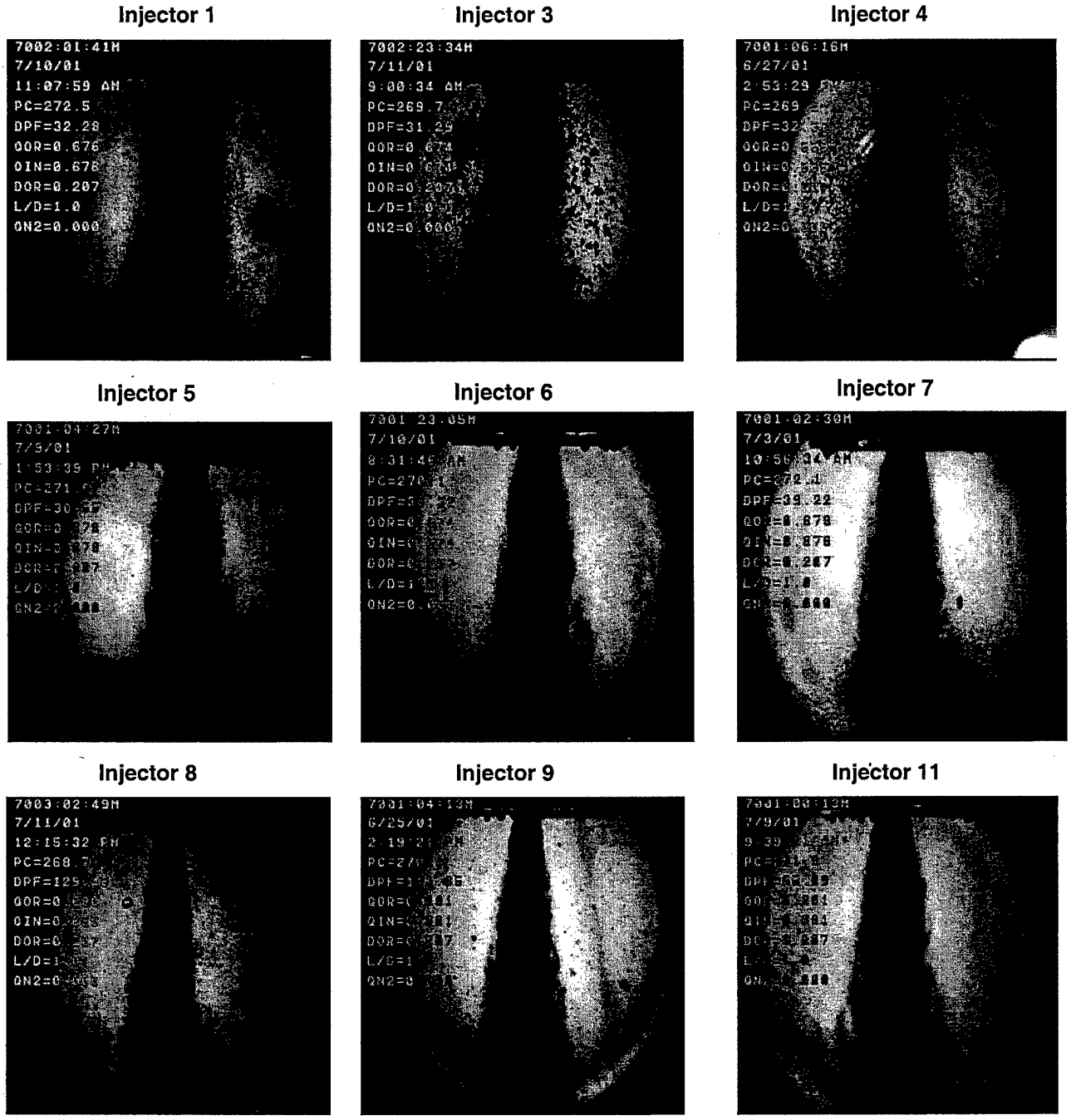

Figure 6: Strobe Back-Lit Images of Nine Elements Operating at an Equivalent Thrust of 333 lb_f

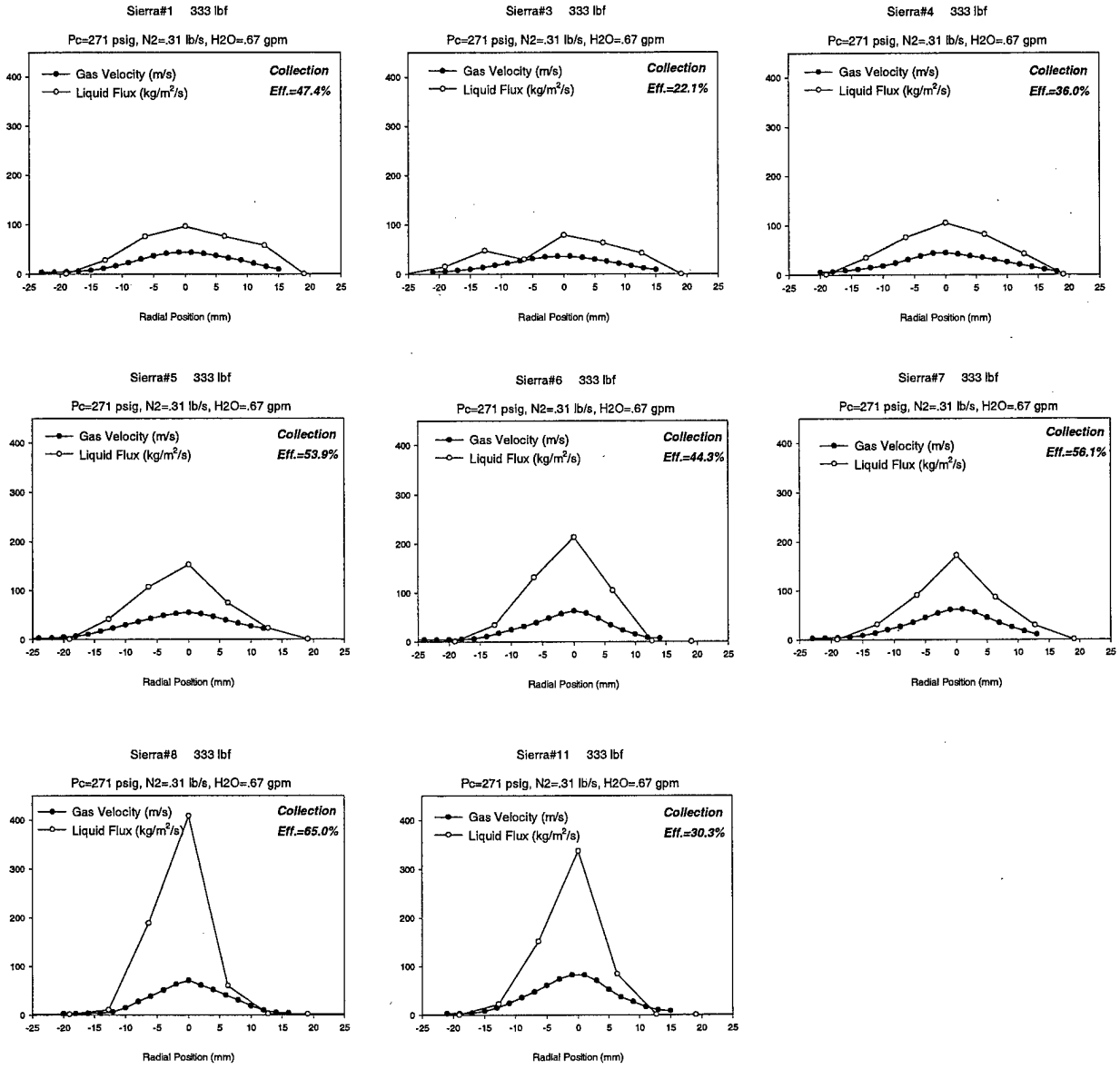

Figure 7: Corrected Liquid Mass Flux and Axial Gas Velocity Profiles for Eight Elements Operating at an Equivalent Thrust of 333 lb_f

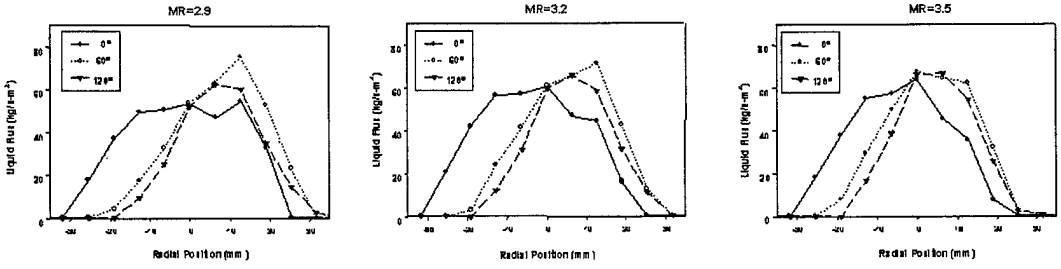

Figure 8: : Influence of Injector Orientation on Measured Gas and Liquid Flux Profiles for Element #3 at Operating MRs of 2.9 (l), 3.2 (c) and 3.5 (r). Operating Chamber Pressure is 857 psi.

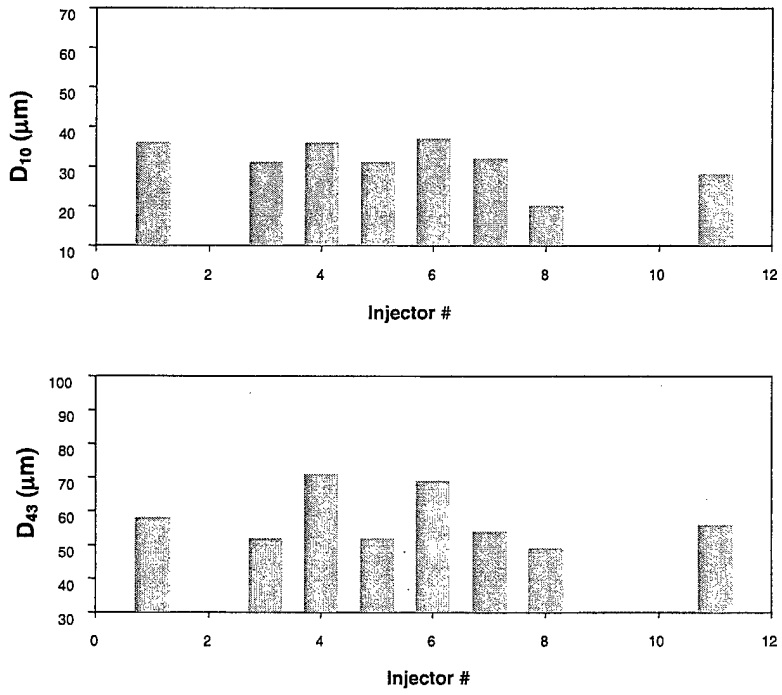

Figure 9: Comparison of D_{10} (top) and D_{43} (bottom) Drop Size Measurements for Elements at 333lb$_f$ Equivalent Operating Condition

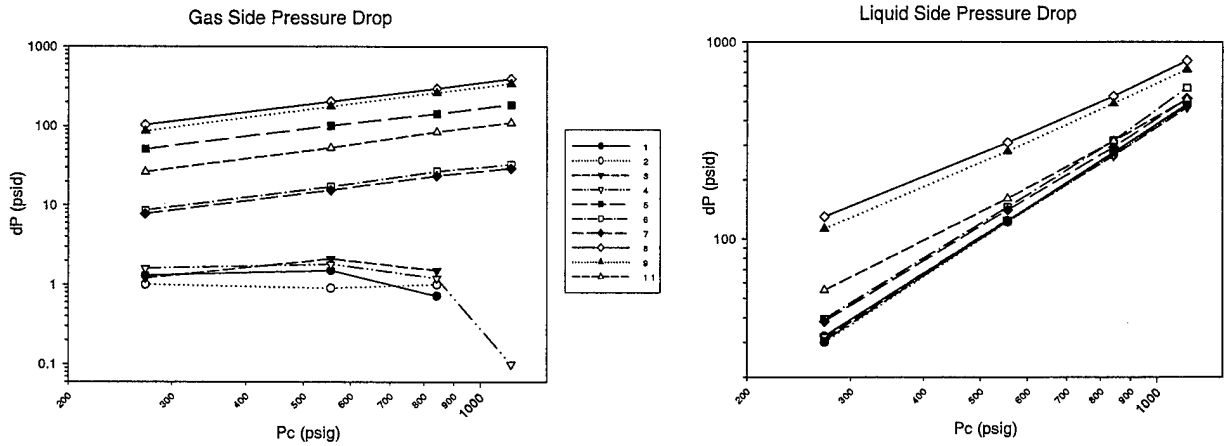

Figure 10: Gas Side (left) and Liquid Side (right) Injection Pressure Drop as a Function of Chamber Pressure

HOT FIRE TEST RESULTS

To date, in excess of 70 successful hot-fire tests have been conducted using the uni-element engine. Additional tests were conducted to determine the ignition timing necessary for these injectors to start smoothly. The elements tested include three divergers (#3, #4 and #5), a pre-filmer (#7) and a converger (#11). The testing thus far has not progressed beyond modest chamber pressures, 200 to 550 psia (Figure 11), significantly lower than the design operating pressures of 750 to 1500 psia. Additional testing at increased chamber pressure is ongoing.

The hot fire data used to characterize the elements include characteristic velocity (C*), heat load and chug stability. Heat load is assessed qualitatively by the temperature of the head-end hardware after the completion of the

test. Chug stability is characterized as "stable or unstable" and a characteristic frequency. Retrospectively, the hot fire performance characteristics are not inconsistent with the cold flow test findings.

The C* efficiency measurements presented are the results from a quick-look analysis of the data. Heat loss to the walls and other losses are not taken into account. However, it is reasonable that these losses will be similar between the different injectors and allows for comparison between the elements. An examination of the random measurement errors shows that, although the error bands for the different injectors do have some overlap, the trends related to injector performance can be seen. The random error in the chamber pressure measurement is ±0.1% of the full scale output of the transducer. This nominally corresponds to ±0.7% of the measured pressure. Flowrates are accurate to ±1% of the measured flowrate for the oxidizer and ±0.4% of the measured value for the fuel. The error in the area measurement is less then ±0.5%. This results in an overall uncertainty less then ±1.4%.

The converger element resulted in the highest C* efficiency, ranging from 91-98% (Figure 12). Qualitatively, this element seems to have the highest head-end heat flux. The C* efficiency increases with increasing MR, and increased oxidizer injection velocity. This injector has shown no signs of chug instability. The cold flow data shows that this element produces a homogeneous, narrow core, which is consistent with high performance. The high injection pressure drop is consistent with chug stable operation.

The pre-filmer element demonstrated significantly lower performance and lower head-end heat loads than the converger element. C* efficiency ranged from 76 to 86%, with little sensitivity to the operating MR. The element has so far only been tested at chamber pressures below 375 psia. At these chamber pressures a chug instability was present with a characteristic frequency of approximately 175 Hz. Additional testing is necessary to characterize the chug stability characteristics at higher operating pressures.

Two diverger elements have been tested so far, #3 and #5. Element #3 has a larger oxidizer post diameter, and therefore lower oxidizer injection pressure drop, than Element #5 (Table 1). Injector #3 also has a 15° divergence angle as compared to Element #5 that has a 0° divergence angle. In the range of pressures tested, Element #3 has a C* efficiency of about 80% independent of operating MR, while Element #5 has a C* efficiency of 81 to 92% increasing slightly with increasing MR. The C* efficiency for this element seems to be more sensitive to chamber pressure then the converging design. As chamber pressure has been increased with this element, the efficiency has also increased. This is consistent with C* efficiency increasing with increasing MR since both result in increased oxidizer injection velocity. Both elements qualitatively appeared to have lower head-end heat loads than the converger element. The low pressure drop diverger, Element #3, is chug unstable at around 175 Hz (approximately 10% peak-to-peak amplitude) for the limited range of chamber pressure tested. It is not believed that this element will be chug stable at higher chamber pressures. The higher pressure drop diverger, Element #5, is chug unstable for chamber pressures below 380 psia. However, it is chug stable at higher chamber pressures. Detailed evaluation of the chug stability data will be used to define design guidelines for the AFT hardware.

SUMMARY

Sierra Engineering and the Air Force Research Laboratory are developing design guidelines for gas-centered swirl coaxial elements. The design methodology is general enough that it can be applied to the development of other novel injector designs. Three basic element concepts have been identified. A set of parametric injection elements has been designed in an effort to identify key design features and acceptable parameter values. Detailed cold flow testing was performed on each of the elements with the hope of identifying remarkable injector characteristics. The cold flow data shows that all the elements produce reasonably uniform mass distributions and atomize extremely well. The injection pressure drop characteristics are more complex than initially assumed, and the hot fire data indicates that this is an important feature for stable operation. At the low pressures tested to date, the element designs appear to have markedly different performance and chug stability characteristics. Ongoing testing will verify these trends, and hopefully identify key design features. As expected in the beginning, the ultimate AFT injection element design will be a compromise of performance, thermal compatibility and combustion stability.

Figure 11: Map of PC-MR Hot Fire Test Conditions

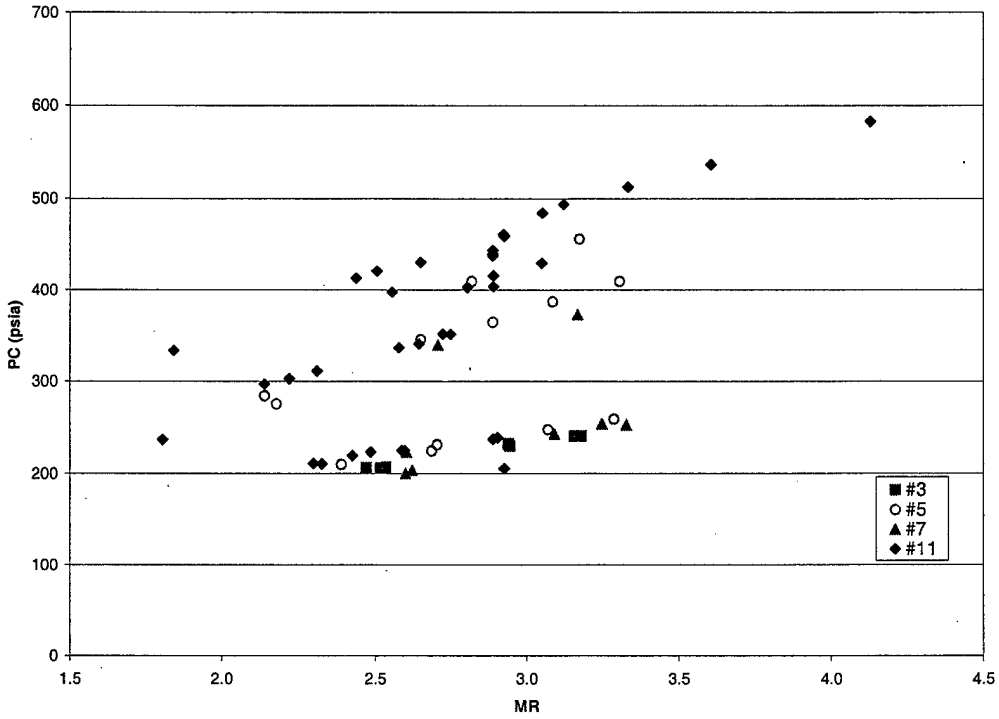

Figure 12: C* Efficiency versus MR for Diverger (#3 and #5), Pre-filmer (#7) and Converger (#11) Elements

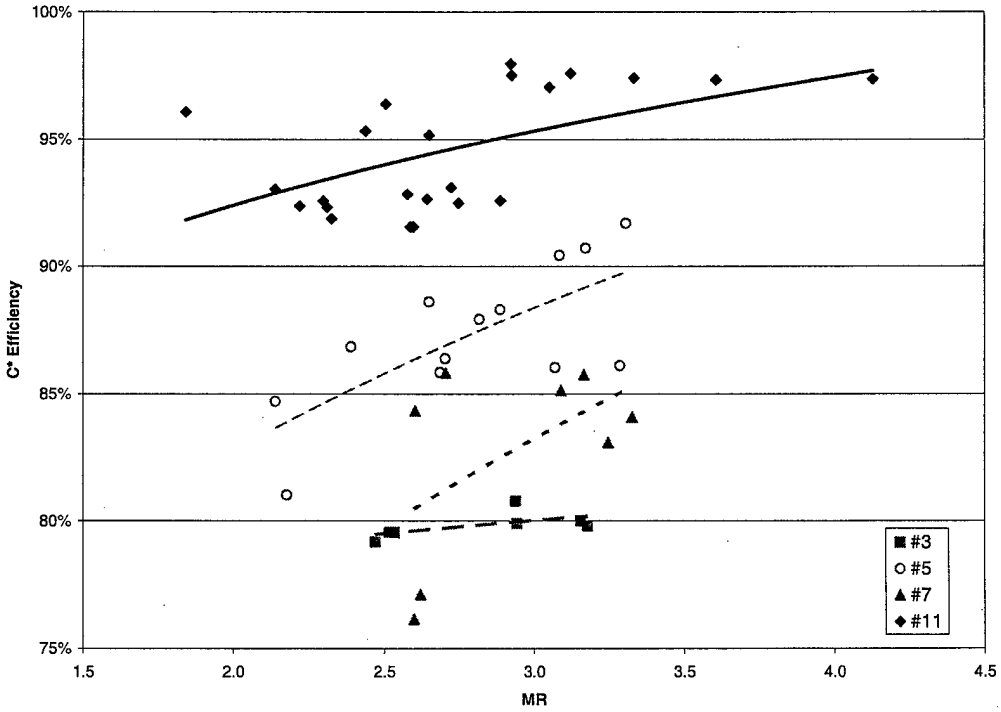

REFERENCES

1. Emission Reduction Through Chemical Kinetic Modeling of Real Engine Effects (REE), Contract F04611-01-C-0010
2. Muss, J.A. and Meagher, G.M.; "Swirl Coaxial Injector Element Characterization for Booster Engines", 1988 Advanced Earth-to-Orbit Propulsion Technology Conference, May, 1988
3. Bailey, T.E, Colbert, J.E. and Mosier, S.A.; FLOX/methane pump-fed engine study, Pratt & Whitney Aircraft, PWA-FR-3040, May, 1969.
4. Oelefein, J.C. and Yang, V.; A Comprehensive Review of Liquid-Propellant Combustion Instabilities in F-1 Engines, Interim Version, Propulsion Engineering Research Center, Penn State University, 23 July 1992.
5. Lefebvre, A.; Atomization and Sprays. Hemisphere Publishing Corp, 1989.
6. Doumas, M. and Laster, R.; "Liquid-Film Properties for Centrifugal Spray Nozzles", *Chemical Engineering Progress*, Vol. 49, No. 10, Oct. 1953.
7. P. A. Strakey, D. G. Talley and J. J. Hutt; "Mixing Characteristics of Coaxial Injectors at High Gas-to-Liquid Momentum Ratios" *Journal of Propulsion and Power*, Vol. 17, No. 2, March-April, 2001.
8. Chehroudi, B., Talley, D.G., and Coy, E.; "Visual Characteristics and Initial Growth Rates of Round Cryogenic Jets at Subcritical and Supercritical Pressures," *Physics of Fluids*, Vol. 14, No. 2, 2002.
9. Cheng, G., Johnson, C.W. and Muss, J.A.; "Swirl Coaxial Injector Development Part II - CFD Modeling", 38th JANNAF Combustion Subcommittee Meetings, Destin, FL, 8-12 April, 2002